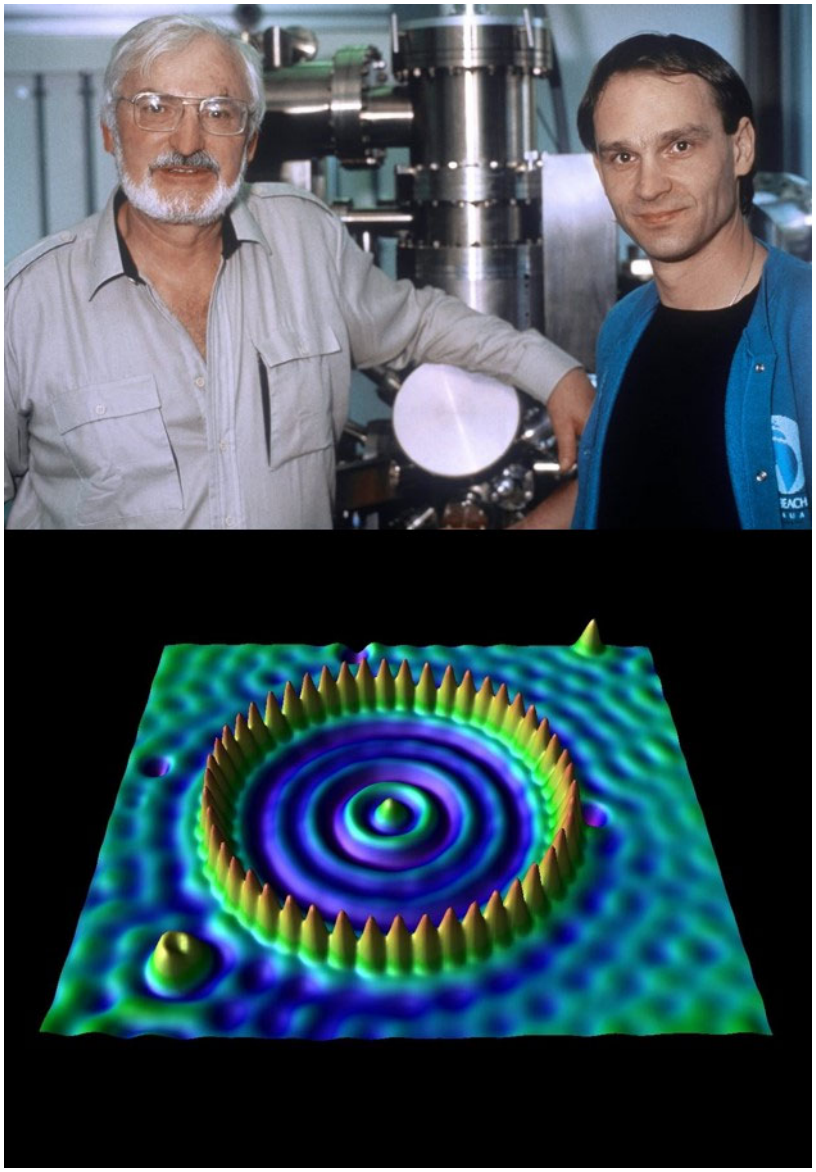

Farming electrons: Scanning Tunnelling Microscopes and Quantum Corrals

Word count: 2993

Introduction

The development of the STM in 1981 by Gerd Binnig and Heinrich Rohrer [1] marked a breakthrough in microscopy and earned them the 1986 Nobel Prize. Previously invented microscopes such as the scanning electron microscope (SEM) presented lower resolution (Fig. 1) and relied on the scattering of electrons off a sample's surface to image this in the reciprocal or Fourier space. The transmission electron microscope (TEM) is capable of even higher resolution than the STM (e.g. recent phase contrast TEM techniques [2]) but is only suitable to image the bulk of a sample. The STM can image surfaces and resolve electronic structures at the atomic scale in real space by means of a long known [3] quantum mechanical phenomenon: quantum tunnelling. In addition, individual atoms may be manipulated allowing for the construction of new electron-confinement structures: quantum corrals.

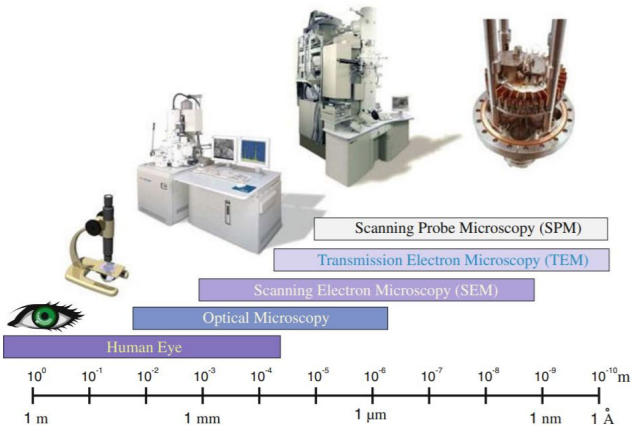

Fig. 1. Imaging resolution of different microscopy techniques [4].

Quantum tunnelling

THEORY

Recalling the first postulate of quantum mechanics is necessary to understand quantum tunnelling. This states that for any dynamical system, such as an electron, the universe, or yourself the reader, there exists a complex-valued probability amplitude known as the wave function that contains all the information on the physical properties of such dynamical system. This wave function is a continuous, single-valued and square-integrable (meaning the indefinite integral of the square of the modulus of the wavefunction is 1) function of the parameters of the dynamical system, including time.

For our purposes, the dynamical system will be an electron, and the wave function describing this electron will be a solution of the time independent Schrödinger equation in one dimension. This wave function, $\Psi(z)$, in a region with zero potential, U, and travelling in the z direction may be written as

$$\Psi(z) = \Psi(0)e^{-ikz}, k = \sqrt{\frac{2m_eE}{\hbar^2}}. \quad (1)$$

Where m_e is the mass of the electron, E is its energy and $\hbar$ is the reduced Planck's constant $\left(\frac{h}{2\pi}\right)$.

Consider a scenario where this travelling electron encounters a potential barrier of total height V_o. In classical mechanics, if $E > V_o$, this particle would have enough energy to propagate over the barrier, but, if $E \leq V_0$ it would not be able to either propagate or penetrate through it as it lacks the energy to do so. We say the region governed by this potential is forbidden in classical mechanics.

In quantum mechanics however, given a narrow and shallow enough potential barrier, this electron with $E \leq V_o$, would be able to penetrate such region and furthermore transmit through it with a finite probability. The electron tunnels through the barrier. What is of special interest in scanning tunnelling microscopy is the form of the wavefunction inside this classically forbidden region as well as the probability of finding an electron within it. This is given by the square of the modulus of the wavefunction in the region's range

$$|\Psi(z)|^2 = |\Psi(0)|^2e^{-2kz}, k = \sqrt{\frac{2m_e(V_o - E)}{\hbar^2}}. \quad (2)$$

We see how the probability depends exponentially on the mass of the particle, the width of the barrier (given by a range in z that the barrier occupies) and its height (given by $V_0 - E$). Therefore, any variations in these, even if small, will cause significant changes in the probability of finding a particle in the classically forbidden region. This is what endows an STM with its incredible sensitivity and ultimately with its atomic vertical resolution as will be depicted next.

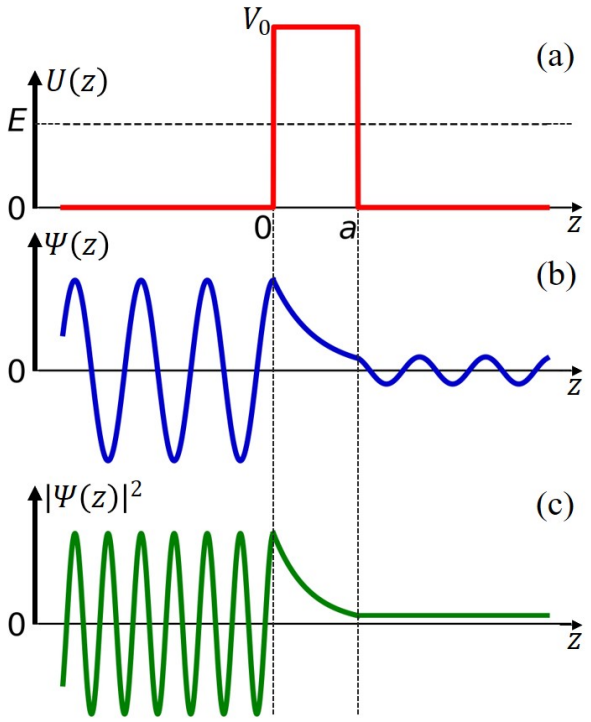

Fig. 2. **(a)**: Potential barrier of total height V_0 (red line) and the energy of an electron E. **(b)**: Electron wave function showing exponential decay inside the barrier and a reduced amplitude in the transmitted wave function to the right of the barrier. **(c)**: Modulus of the wave function squared, i.e. probability of finding an electron along z. To the left of the barrier we have a high reflection probability. Inside the barrier the probability decays exponentially and to the right we have a low transmission probability.

APPLICATION

Analogous to an STM, one of the regions to one side of the potential barrier is a conductive metallic tip used as the STM's scanning probe. The other region to the other side of the barrier is a sample being scanned by this tip, also conductive and typically metallic. The potential barrier is an ultra-high vacuum (UHV) at around 10^{-10} Pa and its total height V_0 is denoted as the vacuum level. Hence, the tip-to-sample distance determines the height of the barrier, $V_0 - E$.

From equation (2), we infer that most of the tunnelling will take place from the last atoms in the tip, or from the surface atoms on the sample, as tunnelling from other atoms will already pose an exponentially significant increase in the distance that electrons will need to tunnel through in the vacuum. That is, an exponentially significant increase in the height of the potential barrier or vacuum level, for this scenario. As a result, the tunnelling probability from these atoms is exponentially less than for the last atoms in the tip (or from the surface atoms on the sample). In fact, tunnelling from just an atom above these will already decrease this probability by around a factor of 150 [4]. In addition, the previously denoted energy of the electron E is limited by the energy of the highest occupied energy level, known as the Fermi level, E_F. This is once again in accordance with what equation (2) describes: even small increases in the width of the barrier, such as having electrons tunnel from lower energy levels, decrease the probability of tunnelling by an exponentially significant amount. As a result, tunnelling from the Fermi level is the most probable.

We have not yet considered however where the transmitted electrons go. In our current configuration, a tunnelling current, i.e. a flow of electrons from the tip to the sample (or from the sample to tip) is not yet possible. The sole reason behind this being that all the energy levels in both the tip and the sample are fully occupied [5]. A potential bias V_b must be applied between these two for some of the energy levels in either the tip or the sample to become unoccupied, so that the tunnelling electron may occupy them thus producing a current. Mathematically, this is more conveniently described by the density of electron (quantum) states per volume per energy that the electrons may take, known as the density of states (DOS) [6]. The direction of the current is determined by the direction of the electric field generated between the tip and sample as depicted with arrows in Fig (3). We furthermore

see that because of the applied potential bias, the potential barrier becomes slightly slanted towards the lower potential.

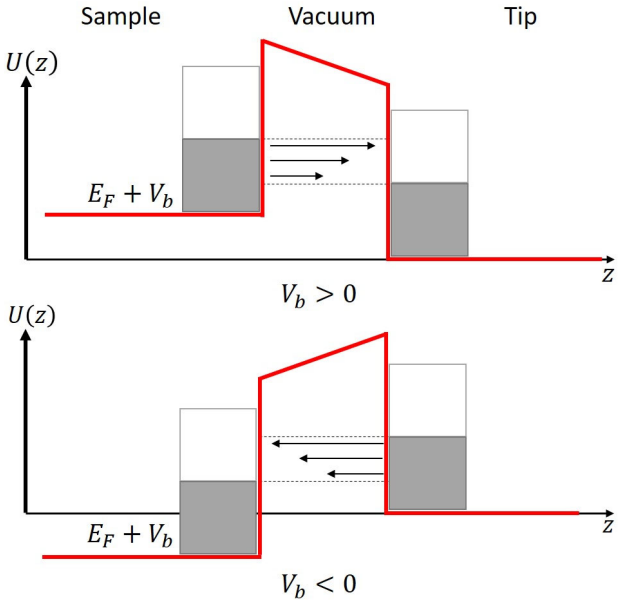

Fig. 3. Schematic of a tunnelling junction with an applied potential bias V_b between the sample and the tip. The grey areas represent occupied electron energy levels and the white areas represent unoccupied electron energy levels. The potential bias raises or lowers the Fermi level in the sample and a tunnelling current flows (arrows). Adapted from [7].

Operation Modes

The STM uses this tunnelling current for its main operation mode: constant-interaction or constant-current mode. In such configuration, the tunnelling current is constantly fed into a feedback loop in the computer, which in turn controls the height of the tip in such a way that the tunnelling current between the tip and the sample is kept constant as the tip scans over the sample. If our sample happens to consist of the same types of atoms (a single element) the DOS will be uniform, and this technique will serve to map the topography of the sample's surface since the tip-to-sample distance will remain constant always. As depicted in Fig. (4), if the tip encounters an atomic step in the sample's surface, the feedback loop will correct for this by increasing the height of the tip such as to maintain the previous tunnelling current. The opposite process applies when the tip encounters a drop in the relief.

The constant height mode is the other common mode of operation. Here the tip is set at a certain height and the tunnelling current is recorded as the tip-to-sample distance varies as the sample is scanned. In comparison to the previous mode, there is a greater chance that the tip may be crashed against the sample when this is translated as no adjustment is made to the tip's height when an atomic step is encountered. In real experiments this is a very common accident.

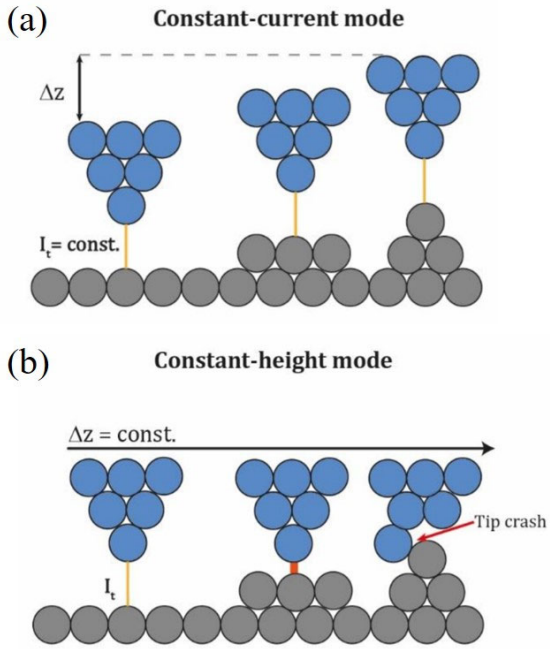

Fig. 4. **(a)**: Constant-current (denoted in the figure as I_t) mode of operation of the tip. **(b)**: Constant-height mode of operation. [8].

Key Components

All previous considerations require that the tip is translated with extraordinary precision. This is achieved using the piezoelectric effect, discovered by Jacques and Pierre Curie in 1880. Certain materials such as piezoceramics (e.g. PZT) will generate an electric charge when mechanical stress is applied on them. Crucially, the inverse procedure is also possible for these special materials: when a voltage is applied across them, they extend or contract depending on the direction of the applied electric field. This is known as the converse piezoelectric effect. These piezoceramics can be stacked to produce piezoelectric drives which may translate the tip

laterally and vertically and jointly form piezoelectric actuators.

The most common and preferred actuator for STMs are piezoelectric tubes (or tube scanners). These present a greater response of around 5 nm/V and simpler operation than tripod scanners as well as being more compact [9]. The tube consists of one inner electrode and four outer electrodes. Stretching along the vertical *z* axis is achieved by applying a voltage between the inner and all four outer electrodes. Lateral bending is achieved by applying a voltage between oppositely facing electrodes. A second attached tube on top of this one corrects for the undesired *z* displacement obtained from laterally bending the tube, which, by itself, has its motion limited to a sphere with radius approximately equal to the length of the tube [4] (instead of a desired plane perpendicular to the tube's axis).

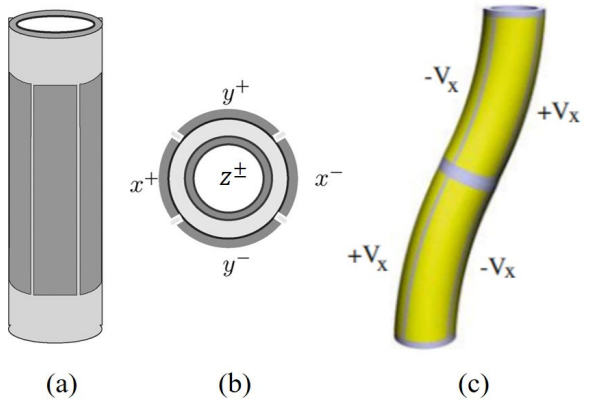

Fig. 5. **(a)**: Side view of a piezoelectric tube actuator. **(b)**: Top view of the piezoelectric tube actuator. Adapted from [10] **(c)**: Two attached tube actuators [4].

The tip is a key component for successful scanning tunnelling microscopy. A blunt tip will end in many atoms from which tunnelling may take place, hence reducing the resolution if not directly precluding the possibility of achieving spatial atomic resolution [11]. A 'bad' tip may also end in two or more minitips rather than a single one, causing tunnelling to take place at a different minitip as the sample is scanned. This leads to inaccurate imaging of the sample's surface structure [12]. An analogy to this would be a digital camera consisting of two or multiple spaced out lenses and a photodiode detector in common for all lenses. When a photo is taken, each lens captures light differently since, although they lie on the same plane, they are each at a different location. This would double or multiply the features of the final image and even distort it as light taken in by each lens would overlap at the camera's photodiode.

The standard procedure for tip etching is through electrochemical etching of tungsten (symbol W) or niobium (symbol Nb). A thin W or Nb wire (typically less than 0.3 mm thick) is submerged a few millimetres into a solution of either a strong acid such as HCl [13] or a strong base such as KOH [12]. A counter-electrode is introduced into this solution to act as the cathode and a current is applied between this and the tip, which acts as the anode. Oxidation at the tip is more prominent just beneath the surface of the electrolyte [12]. This forms a 'neck' in the wire which progressively becomes thinner until it is completely decapitated leaving behind an extremely sharp tip. The current in the external circuit is automatically cut off at that instant. The radii of curvature of the end of this tip are commonly around a few tens of nanometres.

Further necessary refinement of the tips is achieved through cleaning. The etching process and exposure to the air will produce oxides such as WO_3 [12], NbO, NbO_2 or Nb_2O_5 [14]. These act as electrical insulators thereby not allowing stable tunnel currents and hence the need to remove these.

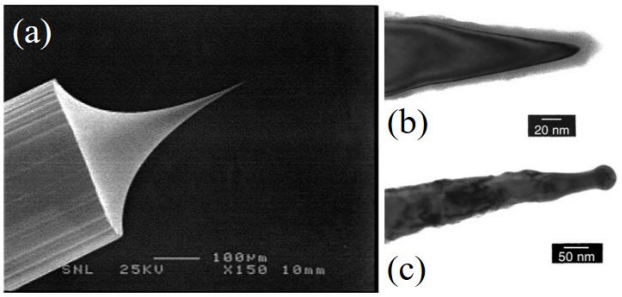

Fig. 6. **(a)**: Etched W tip imaged by a SEM. **(b)**: Untreated electrochemically etched tip imaged by a TEM. An insulating oxide layer of WO_3 is present around the tip. **(c)**: Treated tip with Ar-ion sputtering at 4 keV for 10 min. Oxide layer is no longer present. [12].

Quantum Corrals

The idea that an STM could be used to move atoms using the tip was already contemplated in the early years after the invention of the STM with the impression of an "atomic-scale bit" on a germanium crystal [15].

The theory behind the ability to modify surface structures relies on the fact that strong electric fields can be set between the tip and the sample by applying certain voltage pulses between them. Electromagnetic interactions between the tip and the atoms on the surface of the sample then allow for three main forms of lateral manipulation [8]: a "pulling mode", where the polarity of the voltage is such that an attractive force is formed between the tip and the target atom/s; a "pushing" mode, where the force is repulsive and a "sliding" mode where a more specific interaction allows the tip and the target atom/s to move simultaneously. Finally, atoms may be stripped from the surface, stuck to the tip and redeposited elsewhere, although single atom manipulation using this method requires especially sharp tips [16].

M. F. Crommie *et al.* [17] applied this quality of STMs to the formation of what are known as quantum corrals. These require a sample material containing surface state electrons, i.e. electronic states that exist at the surface of the sample and that are free to move in discrete energy levels [18] within a band gap that contains the Fermi energy [19]. Solutions to the Schrödinger equation for these electrons show that they can only exist on a two-dimensional plane on the surface of the sample since their amplitude decays exponentially both in the direction towards the underlying material and towards the overlying vacuum [19]. In their investigation they proceeded to confine the surface state electrons on a sample of Cu(111) in a ring of Fe atoms (which are therefore described more appropriately as Fe adatoms) positioned using the "sliding" mode of the tip. Given the ring has a diameter that is comparable to the surface state electron's de Broglie wavelength, these will exhibit quantum mechanical behaviour [5]. One of these behaviours is of course that electrons behave as

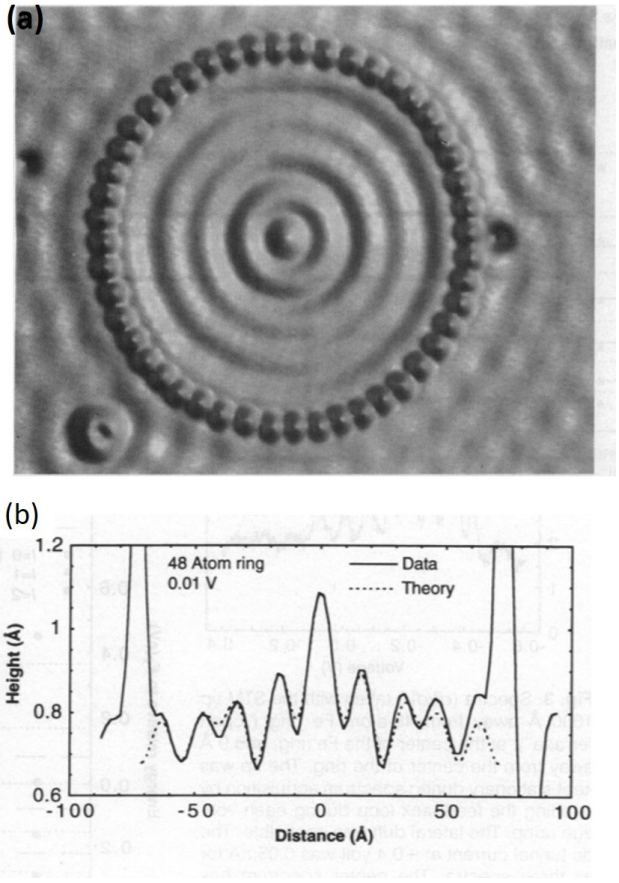

Fig. 7. (**a**): Quantum corral constructed from 48 Fe adatoms on a defect-free surface of Cu(111) ($V_b = 0.01\,V, I_t = 1.0\,nA$). (**b**): Data (solid) and fitted curve (dashed) for the tip height along the cross section of the quantum corral, which had a diameter of 142.6 Å. Note in this paper, the distribution outisde the ring could not be accounted for by the theory with accuracy. [17].

matter waves and as such may scatter from the Fe adatoms and interfere with one another.

These effects were described by E. J. Heller *et al.* [20] one year after the first publication on quantum corrals. Let us imagine that the tip is initially placed at the centre of the ring. If a bias voltage is applied between the tip and the Cu(111) sample, given an appropriate polarity, electrons will tunnel from the tip onto the Cu(111) surface. These electrons may then be regarded as surface state electrons that, behaving like waves, will propagate towards the confining Fe adatoms and will scatter from these. After one scatter (if the wave is incident normal to the scattering centre of an Fe adatom) or multiple scattering from many Fe adatoms, the wave will end up propagating through the centre of the ring (where the tip lies). This wave will interfere with

the incoming electrons from the tip, which may also be regarded as waves, generating standing-wave patterns. The interference causes fluctuations in the DOS across the surface and hence fluctuations in the tunnelling current. This can be measured and fed to the STM's feedback loop to adjust the tip's height in the constant current mode. If the tip is then translated to another location, a complete distribution of the tip's height as a function of position can be obtained for the confined circular area as well as the surroundings (Fig. 7).

Cu(111) was chosen as the sample material because, like other noble metals, Cu(111) is made from a crystalline lattice such that when it is cut at a particular orientation, surface state electrons remain on the flat surface generated by the cut. On the other hand, the choice of Fe adatoms is justified due to its scattering properties. In [17] the scattering strength of Fe adatoms for surface state electrons at the Fermi energy is quantified as a phase shift in the scattered wave of -80° ± 5°, which is considered strong scattering. Later in [20], a more accurate interpretation of the Fe adatom scattering was given and a corrected phase shift of 90° was calculated. In this paper the scattering was determined to be absorptive rather than completely elastic as presented in previous work [17]. The consequence of this is that half of the energy of the electron waves is absorbed into the Cu(111) bulk and only 25% is reflected. The remaining 25% was found to be transmitted, which was in accordance with the previously unexplained density distributions seen outside the confining ring in [17].

Researchers continue to explore the physics of confined electrons by quantum corrals and their many variations. Other confining shapes have been considered already such as triangles, squares, stadiums [21] or ellipses [22]. These last two play an important role in present studies of quantum chaos and quantum mirages, respectively.

Bibliography

Cover page:

Top image: Douglas Martin. Heinrich Rohrer, Physicist, Dies at 79; Helped Open Door to Nanotechnology. *The New York Times.* May 21st 2013. Available from: https://www.nytimes.com/2013/05/22/science/heinrich-rohrer-physicist-who-won-nobel-dies-at-79.html?smid=em-share [Accessed 4th January 2021]

Bottom image: Dr. Don Eigler. *Building Things with Atoms: A Report from the Small Frontier*. [Public Lecture] IBM, Almaden Research Center. 12th December 2001.

[1] G. Binnig, H. Rohrer. Scanning tunneling microscopy. *Surface Science.* 1983; 126 (1): 236-244. Available from: https://doi.org/10.1016/0039-6028(83)90716-1 [Accessed 21st December 2020]

[2] Yücelen E, Lazić I, Bosch EGT. Phase contrast scanning transmission electron microscopy imaging of light and heavy atoms at the limit of contrast and resolution. *Scientific reports.* 2018; 8 (1): 2676-10. Available from: https://www.ncbi.nlm.nih.gov/pubmed/29422551.

[3] Eugen Merzbacher. The Early History of Quantum Tunneling. *Physics Today.* 2002; 55 (8): 44-49. Available from: https://doi.org/10.1063/1.1510281 [Accessed 21st December 2020]

[4] Voigtländer, Bert. (2015) *Scanning Probe Microscopy*. Berlin, Heidelberg: Springer-Verlag. Available from: https://ebookcentral.proquest.com/lib/[SITE_ID]/detail.action?docID=1998099. [Accessed 2nd December 2020]

[5] David O. Hayward, E W. Abel ed. *Quantum Mechanics for Chemists*. Cambridge, UK: Royal Society of Chemistry; 2002. Available from: https://doi.org/10.1039/9781847551801-00048 [Accessed 22nd December 2020]

[6] Cosme Gonzalez Ayani. Interviwed by: Pablo Garcia Aragoneses. 28/12/2020

[7] Lab Manual. University of Washington. 2009

[8] Sánchez Grande, Ana. Design and characterization of functional nanomaterials on surfaces. PhD thesis. Autonoma University of Madrid, 2020.

[9] G, Smith DPE. Single-tube three-dimensional scanner for scanning tunneling microscopy. *Review of Scientific Instruments*. 1986; 57 (8): 1688-1689. Available from: doi: 10.1063/1.1139196 Available from: https://doi.org/10.1063/1.1139196 [Accessed 22nd December 2020]

[10] Aphale S, Fleming AJ, Moheimani SOR. High speed nano-scale positioning using a piezoelectric tube actuator with active shunt control. *Micro & nano letters*. 2007; 2 (1): 9. Available from: https://search.proquest.com/docview/1636191201 [Accessed 29th December 2020]

[11] Hockett LA, Creager SE. A convenient method for removing surface oxides from tungsten STM tips. *Review of Scientific Instruments*. 1993; 64 (1): 263-264. Available from: doi: 10.1063/1.1144394 Available from: https://doi.org/10.1063/1.1144394 [Accessed 22nd December 2020]

[12] Inger Ekvall, Erik Wahlström, Dan Claesson, Håkan Olin, Eva Olsson. Preparation and characterization of electrochemically etched W tips for STM. *Measurement Science and Technology*. 1999; 10 (1): 11-18. Available from: https://doi.org/10.1088/0957-0233/10/1/006 [Accessed 23rd December 2020]

[13] Eder G, Schlögl S, Macknapp K, Heckl WM, Lackinger M. A combined ion-sputtering and electron-beam annealing device for the in vacuo postpreparation of scanning probes. *Review of Scientific Instruments*. 2011; 82 (3): 033701. Available from: doi: 10.1063/1.3556443 Available from: https://doi.org/10.1063/1.3556443 .

[14] Ternes, Markus. Scanning tunneling spectroscopy at the single atom scale. PhD thesis. École Polytechnique Fédérale de Lausanne, 2006.

[15] Becker, R., Golovchenko, J. & Swartzentruber, B. Atomic-scale surface modifications using a tunnelling microscope. *Nature*. 1987; 325: 419–421. Available from: https://doi.org/10.1038/325419a0 [Accessed 24th December 2020]

[16] In-Whan Lyo, Phaedon Avouris. Field-Induced Nanometer- to Atomic-Scale Manipulation of Silicon Surfaces with the STM. *Science*. 1991; 253 (5016): 173-176. Available from: https://doi.org/10.1126/science.253.5016.173 [Accessed 24th December 2020]

[17] M. F. Crommie, C. P. Lutz, D. M. Eigler. Confinement of Electrons to Quantum Corrals on a Metal Surface. *Science*. 1993; 262(5131), 218-220. Available from: https://doi.org/10.1126/science.262.5131.218 [Accessed 24th December 2020]

[18] Forstmann F. The concepts of surface states. *Progress in Surface Science*. 1993; 42 (1): 21-31. Available from: http://www.sciencedirect.com/science/article/pii/007968169390055Z [Accessed 24th December 2020]

[19] Fiete GA, Heller EJ. Colloquium: Theory of quantum corrals and quantum mirages. *Reviews of modern physics*. 2003; 75 (3): 933-948. Available from: https://search.datacite.org/works/10.1103/revmodphys.75.933 [Accessed 25th December 2020]

[20] E. J. Heller, M. F. Crommlett, C. P. Lutzt & D. M. Elglert. Scattering and absorption of surface electron waves in quantum corrals. *Nature*. 1994; 369: 464-466. Available from: https://doi.org/10.1038/369464a0 [Accessed 25th December 2020]

[21] Crommie MF, Lutz CP, Eigler DM, Heller EJ. Quantum corrals. *Physica D: Nonlinear Phenomena*. 1995; 83 (1): 98-108. Available from:http://www.sciencedirect.com/science/article/pii/016727899400254N [Accessed 28th December 2020]

[22] Li, Q., Li, X., Miao, B. *et al.* Kondo-free mirages in elliptical quantum corrals. *Nat Commun*. 2020; 11(1): 1400. Available from: https://doi.org/10.1038/s41467-020-15137-8 [Accessed 29th December 2020]